

# Edge Detection of Noisy Images Using the Intelligent Techniques

Hamid Reza Alikhani<sup>1</sup>, Ali Reza Naghsh<sup>2</sup>, Razieh Jalali Varnamkhashti<sup>3</sup>

1- Tafresh University/Electrical Department, Tafresh, Iran.

Email: alikhani.hamid@gmail.com (corresponding author)

2- Najaf Abad Azad University/Electrical Department, Najaf Abad, Iran.

Email: naghsh\_ali@yahoo.com

3- Tafresh University/Electrical Department, Tafresh, Iran.

Email: raziehalali89@yahoo.com

Received: June 2012

Revised: August 2012

Accepted: October 2012

## ABSTRACT:

In this paper an approach is presented for edge detection of noisy images that have been degraded by impulsive noise. It uses Fuzzy Inference System (FIS) and Ant Colony Optimization (ACO). Starting with, using the FIS with 12 simple rules is to identify the noisy pixels in order to perform the filtering operation only for the noisy pixels. Probable edge pixels in 4 main directions for filtered image are detected using fuzzy rules and then ACO is applied by assigning a higher pheromone value for the probable edge pixels rather than other pixels so that the ant's movement toward edge pixels gets faster. Another factor is the influence of the heuristic information in the movement of any ant that is considered to be proportional to local change in intensity of each pixel in order to the possibility of movement of ants increased toward pixels that have more change in their local intensity. Finally, by using an intelligent thresholding technique which is provided by training a neural network, the edges from the final pheromone matrix are extracted. Experimental results are provided in order to demonstrate the superior performance of the proposed approach.

**KEYWORDS:** ant colony optimization, edge detection, noisy image, fuzzy system.

## 1. INTRODUCTION

Noise reduction and edge detection of images are two of the most important concepts in the field of computer vision and image processing. Images are usually corrupted by usage of noisy sensors, error of transmission channel or storage hardware. Keeping the structure of the image is one of the most important points in recovery and improvement of the damaged images. Until now many methods have been presented for noise reduction in various books and articles [1] – [3]. Using of the simple filters such as median filter, average filter and Gaussian filter is one of the methods for noise reduction but these filters despite of the noise reduction tend to smooth and blurred images [3]. This is important that various median filters have the same behavior for all image's pixels, including healthy pixels and noisy pixels. In recent years new methods are provided to reduce the impact of filtering on the healthy pixels. These methods consist of two steps: identification of noisy pixels is performed in the first step and in the second step the filtering operation is performed for noisy pixels only. A method based on the two steps process is Tri-State Median Filtering (TSM) [4]. This filter comprises of Standard Median (SM)

filter, identity filter, Center Weighted Median (CWM) filter and a switching logic. Noise detector takes the outputs from the standard median filter and center weighted median filter and compares them with the center pixel value in order to detect the noise. The switching logic is controllable by a threshold value. This threshold value determines the center pixel value to have the value of a filter from mentioned filters. Pixel-Wise MAD (PWMAD) is another technique based on modified median of absolute deviation from median (MAD). An iterative pixel wise modification of MAD is used in [5] that provide the elimination of noise with an amplified computational cost. Rank-Ordered Absolute Difference (ROAD) is another method for noise reduction that measures the closeness of a test pixel with its neighboring pixels [6]. Reference [7] shows another method for noise reduction by using a neural network. This method uses of PWMAD and ROAD parameters. In this case having the information of healthy image is necessary for the initial training of the neural network. As mentioned, Edge detection is an important area of image processing and since the images are generally contaminated with noise, edge detection investigation in a noisy condition has a

significant importance. The main aim of edge detection of a digital image is to find and illustrate the objects in an image. There are many applications in the industries, such as image processing (wildly used in medicine), computer vision and so on. In the last decade many methods have been proposed in the area of edge detection. One of the techniques mostly used in edge detection is in taking advantage of linear-time-invariant (LTI) filters which have little calculation complexity in computation [3]. In the first order of filters any abrupt changes in the pixels intensity between two neighboring pixels is called to be an edge and therefore the pixels in the image which have its derivative value (amplitude) of the gray level intensity to be high, is considered to be an edge [3]. In spite of the vast usage of these filters in edge detection, one cannot get good results once we are dealing with the images with non-uniform lighting [8]. Usage of second-order derivative is one of the traditional approaches for edge detection that is rarely used; it is because the second-order derivatives are highly sensitive to noise. The Laplace value produces a doubling edge effect which is not acceptable [3]. However, Laplacian can be a powerful complementary in combination with the other edge detection techniques. In recent years, the temptation and tendency of using intelligent techniques for edge detection among the researchers is increased in order to overcome the drawbacks of traditional methods. The FIS is presented for edge detection by considering the edge continuity. It also works well with noisy images. However, the increase in the noise level will degrade the results, this is because of the fact that as the noise level increases, the noise pixels become connected, and they lose their randomness [9]. Another type of fuzzy edge detector is presented in which all inputs to the FIS are obtained by applying the original image to a linear high-pass filter, a first-order edge detector filter (Sobel horizontal and perpendicular operators), and a low-pass filter. Then the output of the operators is used as the input to the fuzzy inference system [8]. This method according to the simulation of [8], in a non-uniform lighting condition gives an acceptable solution for the images and prevents the double edge effect. An edge detection algorithm employing multi-state adaptive linear neurons has been presented which can reduce the noise effect without increasing the mask size. The inputs are defined using the local mean in a predefined mask of  $3 \times 3$  and then the one-dimensional edges are defined so that they are linearly separable from the non-edges. This technique needs a vast computational effort [10]. Reference [11] shows that by using a recurring neural network, a general solution for the edge detection is presented. There are three outputs for each pixel of the input image at network where two of these outputs represent discontinuities in horizontal and vertical directions and the third one separates the edge

pixels from non-edge pixels. However, this method has great computational effort and as the image size increases, the number of neurons in neural network increases monotonically. As an example, for an image with  $128 \times 128$  pixels a neural network with  $3 \times 128 \times 128$  is needed. ACO is one of the heuristic approaches that has many applications [12]-[17] and is applied to edge detection problem in this paper. The biological origination of this algorithm refers to depositing of pheromone that ants leave on the ground while moving. Through smelling these chemicals, ants use it for exchanging the information about routes and choose the appropriate path. Each ant that moves on an inoculated path with pheromone strengthens the pheromone on the path with their pheromone. This positive feedback mechanism finally leads the ants to follow the best paths after a transient time. Dorigo proposed the first ACO model, Ant System (AS) in 1991 for solving the Travel Salesman Problem (TSP) in a small dimension. AS is divided into three models; Ant Cycle (AC), Ant Quantity (AQ) and Ant Density (AD), according to the update time of the pheromone [18]. Since then, a large number of extensions have been developed to AS such as the Ant Colony System (ACS) [19] and Max-Min Ant System (MMAS) [20]. Reference [21] shows that the ACO is used for edge detection problem. This work is performed by employing the special functions for heuristic information and using the thresholding technique named Otsu technique [22]. Experimental results in [21] show that this method does not have the ability of extracting the edges completely. Another usage of the ACO for edge detection is introduced in [23]. This method has employed the composition of AS and ACS models and benefits from performing the Daemon operations. The method that is proposed in [24] exploits the AS model for edge detection in which further adjustment to refine the edge (morphological thinning operation) is done as a post-processing. Another approach based on Ant Colony Optimization is proposed in [25] that combine the gradient and relative difference of statistical means for the ant's searching.

In our paper a new method is proposed to reduce the noise of image by using the capabilities of FIS and exploiting the ROAD and Absolute Deviation from Median (ADM). The performance of this method is to evaluate by PSNR criterion. Then ACO is employed to edge detection for the image that is filtered by fuzzy filtration. For updating pheromone similar to ACS model, it uses both local and global updating, however the state transition rule is introduced by introducing a new innovation at the state transition rule of AS. This new innovation is so that the ants are directed to the edges with higher probability.

The rest of our paper is organized as follows: in section 2, a noise reduction method is presented. Then,

an image edge detection approach is presented in section 3. Simulation results are presented in section 4. Finally, section 5 covers the conclusion of this paper.

**2. NOISE REDUCTION APPROACH**

The presented method for noise reduction is based on estimating-removed strategy. The FIS determines whether the pixel is noisy or not and assigns a degree to each pixel. This work is performed by defining the membership functions for two parameters ADM and ROAD and using of rules that human knowledge defines them. Degree of each pixel is a real number in the interval [0, 1] that shows the probability of a pixel being healthy.

**2.1. Absolute Deviation from Median**

If  $c_{ij}$  displays a pixel with coordinates (i, j) in noisy image and  $C_{ij}$  is a matrix centered around  $c_{ij}$  within a  $(2N + 1) \times (2N + 1)$  size window ( N is equal to 3 in this paper), then  $m_{ij}$  that represents the pixel with coordinate(i, j) in median image is obtained from equation in (1).

$$m_{ij} = median(C_{ij}) \tag{1}$$

According to these definitions, the absolute deviation between the noisy image and median image at each pixel with coordinate(i, j) is expressed by (2).

$$ADM_{ij} = |c_{ij} - m_{ij}| \tag{2}$$

**2.2. Rank-Ordered Absolute Difference**

Where, at noisy image,  $C_{ij}$  is a matrix centered around  $c_{ij}$  within a  $(2N + 1) \times (2N + 1)$ size window. In this neighborhood,  $C^{(out)}$ is the pixels around the centered pixel  $c = c_{ij}$ ; then for each pixel  $d \in C^{(out)}$ , the absolute difference between gray value I of the pixels d and c as defined in (4).

$$S_{c,d} = |I_c - I_d| \tag{4}$$

Therefore for each pixel, there are eight values of  $S_{c,d}$  which are sorted in ascending form, that is:

$$S_{c,d}^{(q)} \leq S_{c,d}^{(q+1)}, q = 1, 2, \dots, 7.$$

Hence, the Rank-Ordered Absolute Difference (ROAD) is defined as:

$$ROAD_m(c) = \sum_{q=1}^m S_{c,d}^{(q)} \tag{5}$$

Where,  $2 \leq m \leq 7$ . In our simulation m is taken to be 4 in order to determine  $ROAD_4(c)$ . This statistical

figure provides a measure of how close a pixel value is to its four neighbor pixels.

**2.3. Fuzzy System and Noise Reduction Algorithm**

A brief noise reduction algorithm as follows:

- a) The value of ADM is calculated for each pixel of image.
- b) The value of ROAD is calculated for each pixel of image.
- c) FIS assigns a degree to each pixel in the interval [0, 1] by using of the two input parameters ADM and ROAD and the fuzzy rules.
- d) The value of pixels that FIS has identified them as noisy pixels is replaced with the mean value of neighboring pixels.

FIS uses triangular and trapezoidal membership functions for input and output parameters. Fig. 1 shows this membership functions and corresponding linguistic variables.

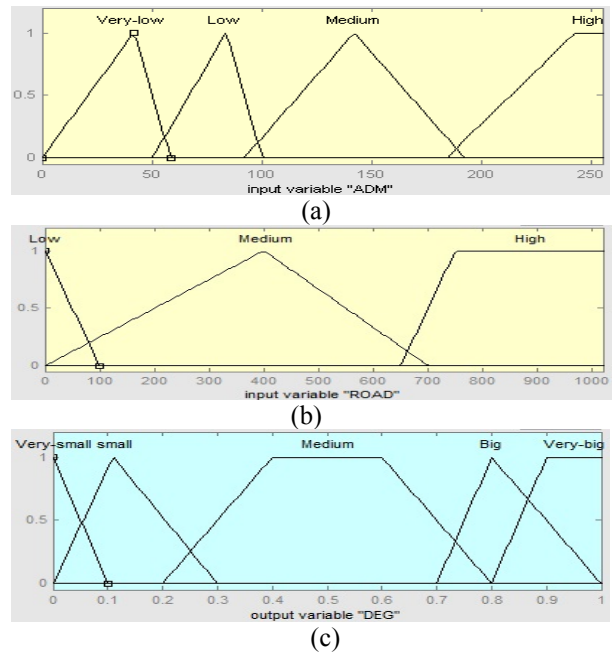


**Fig.1.** (a) Membership functions for ADM. (b) membership functions for ROAD. (c) Membership functions for output.

Since the range of input image is in interval [0, 255], the range of ADM is in interval [0, 255] too but we cannot be sure that the range of ROAD is in the same range. We have used  $ROAD_4(c)$  and maximum difference between intensity of two pixels is not more than 255, so the interval [0, 1020] is suitable for ROAD parameter. FIS assigns a degree to each pixel in interval [0, 1] by definition 12 rules that are listed in Table. 1. Rules have been set so that each healthier pixel has its assigned degree closer to one and vice versa for the

noisier pixels the filtering operation is performed with smaller degree.

**Table 1.** Fuzzy rules

ADM \ ROAD	Very-Low	Low	Medium	High
Low	Very-Big	Very-Big	Very-Big	Very-Big
Medium	Very-Big	Big	Medium	Medium
High	Big	Medium	Small	Very-small

**3. ACO BASED IMAGE EDGE DETECTION**

In this paper, we used combinational structure of the FIS, ACO and neural network for the image edge detection.

**3.1. Identification of Possible Edges Using FIS**

We use a simple fuzzy system for identification of the edge of the pixels before setting the parameters of the ACO. This is done so that one can distinguish between the edge of the pixels and the rest of pixels in adjusting the parameters in order to have the movement of the ants directed toward the edges in a directional manner. Fuzzy system detects the edges in 4 main directions by utilizing 4 simple rules. For 3 × 3 neighborhood shown in Fig. 2, the difference between the intensity of the central pixel G and its neighboring pixels is calculated according to (6) and then, they form the inputs of the fuzzy system.

$$x_i = I_i - I_G \quad , \quad i \in \{1, 2, \dots, 8\} \quad (6)$$

Where  $I_G$  is the intensity value of the central pixel G, and  $I_i$  is the intensity value of the neighbor pixel  $i$ .



**Fig. 2.** Illustration of 3x3 neighborhoods.

Trapezoidal membership functions are used for all of the inputs as shown in Fig. 3. One should notice that the intensity value of the pixels for the input image is in the interval [0, 255], and the input of fuzzy system will be in the interval [-255,255].

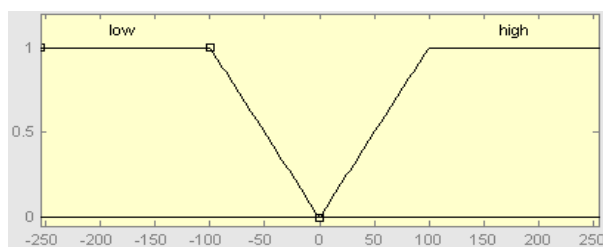


**Fig. 3.** Membership function of the input variable  $x_i$ .

Based on input membership functions, four rules are defined for identification of the edges which are listed in Table. 2.

**Table 2.**Fuzzy rules for identification the edge pixels.

	Low	High	None	Edge
Rule(1)	$x_1, x_7, x_8$	$x_3, x_4, x_5$	$x_2, x_6$	G
Rule(2)	$x_1, x_2, x_3$	$x_5, x_6, x_7$	$x_4, x_8$	G
Rule(3)	$x_1, x_2, x_8$	$x_4, x_5, x_6$	$x_3, x_7$	G
Rule(4)	$x_6, x_7, x_8$	$x_2, x_3, x_4$	$x_1, x_5$	G

Rules (1) and (2) are identified for horizontal and vertical edges, respectively and two other rules are to detect the edges in diagonal directions. For example the third law states that if the inputs  $x_1$ ,  $x_2$ , and  $x_8$  are in low membership function and the  $x_4$ ,  $x_5$ , and  $x_6$  are in high membership function then the probability that the central pixel and the pixel 3 and 7 in Fig.2 are along an edge.

**3.2. Proposed Method for Image Edge Detection Based on ACO.**

Ant's algorithm can be used for solving the discrete optimization problems in which their space solution is discrete. A two dimensional digital image with the size  $M \times N$  can be defined as a discrete space of pixels. This discrete space can be represented by a graph that graph nodes are image pixels and graph connections are done by connecting the adjacent pixels together as in Fig. 4.

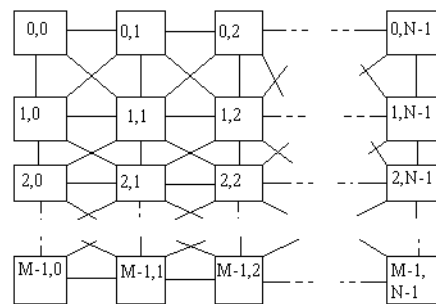


**Fig. 4.** Graphicalrepresentation of an image.

In order to start the edge detection by ACO, the first stage is setting the initial value of parameters. The important parameters that should be set are the pheromone value assigned to each pixel and the heuristic information of the pixels. In all the previous works, a small number that is close to zero is considered as the initial value of the pheromone for all the pixels but in our paper the initial value of the pheromone that is assigned to the identified edge pixel by fuzzy system is more than of pheromone value of the rest of the pixels. This difference in pheromone

value causes to create a pre-understanding for the movement of the ants. This means that in the beginning of task it seems that the ants have already passed through the edge pixel and have increased the amount of pheromone for those pixels. This causes the ants to move toward the edge pixels more. The manner that the initial pheromone assigned to pixels is expressed by (7).

$$\tau_{ij} = \begin{cases} \tau_{\max} & \text{if } (i, j) \text{ is possible edge} \\ \tau_{\min} & \text{if } (i, j) \text{ is nonpossible edge} \end{cases} \quad (7)$$

Where,  $\tau_{ij}$  is the pheromonevalue for the pixel(i, j).

Note that in this step, the probable edge pixels are determined and it isn't the edge detection performance because many of those probable edge pixels may not be really part of edge pixels, or number of actual edge pixels cannot be detected with this simple analysis. The result of this step for the standard image of Lena is shown in Fig. 5 that confirms the mentioned statements.



Fig. 5. Resulted probable edge pixels for Lena image.

Another important parameter is heuristic information matrix which is made based on local changes in the pixels intensity and its value at pixel (i, j) is determined by (8).

$$\eta_{ij} = V_c(I_{ij}) \quad (8)$$

Where,  $I_{ij}$  is the intensity value of the pixel at (i, j) in the normalized image,  $V_c(I_{ij})$  is a function that operates on the neighboring pixels around the pixel(i, j). It depends on the variation of the intensity values on the local neighborhood and is expressed as follow:

$$V_c(I_{ij}) = f \left( \begin{matrix} |I_{i-1,j-1} - I_{i+1,j+1}| + |I_{i-1,j} - I_{i+1,j}| + \\ |I_{i-1,j+1} - I_{i+1,j-1}| + |I_{i,j-1} - I_{i,j+1}| \end{matrix} \right) \quad (9)$$

To determine the function  $f(\cdot)$  in (9), an exponential function is considered in this paper and its mathematical form is according to the (10).

$$f(x) = 0.1e^x \quad (10)$$

In this paper, the coefficient of 0.1 is obtained by trial and error method.

After adjusting the initial value of the parameters, K numbers of ants become randomly distributed on the graph. On every iteration, each ant moves across the image, from one pixel to another, until it has made L construction steps (L is called the number of the construction steps). Each ant moves according to the amount of pheromone and heuristic information related to the neighboring pixels of the current position in the format of the state transition law. Each ant updates the pheromone value of visiting the arcs (linking the neighboring nodes) based on the local updating rule. At the end of the each iteration, after all ants finished the construction process, some amount of pheromone is updated on special arcs based on global update rule. Fig. 6 shows the general structure of the ACS that is used in our paper. The state transition rule of our paper is different from the rules of AS that is expressed in (11). According to (11), on  $n^{\text{th}}$  construction process, the  $k^{\text{th}}$  ant moves from pixel at  $(i_0, j_0)$  to pixel at (i, j) based on transition probability  $P_{(i_0, j_0)(i, j)}^{(n)}$ .

$$P_{(i_0, j_0)(i, j)}^{(n)} = \frac{(\tau_{ij}^{(n-1)})^\alpha (\eta_{ij})^\beta}{\sum_{(i, j) \in \Omega_{(i_0, j_0)}} (\tau_{ij}^{(n-1)})^\alpha (\eta_{ij})^\beta} \quad (11)$$

where,  $(i_0, j_0)$  is the current position of the ant; (i, j) is the next position for the ant;  $\tau_{ij}$  is the pheromone value for pixel (i, j);  $\Omega_{(i_0, j_0)}$  is the neighborhood pixels of pixel  $(i_0, j_0)$ ;  $\eta_{ij}$  is the heuristic information at pixel(i, j); and the constants  $\alpha$  and  $\beta$  control the influence of the pheromone and the heuristic information, respectively.  $\sum_{(i, j) \in \Omega_{(i_0, j_0)}} (\tau_{ij}^{(n-1)})^\alpha (\eta_{ij})^\beta$  is a normalization factor to limit the values of  $P_{(i_0, j_0)(i, j)}^{(n)}$  in [0, 1]. In fact, this law is the balance between the heuristic part and the pheromone trial. The heuristic information emphasize the selection of closer pixels with higher change in their intensity, whereas, pheromone trial emphasizes the selection of arcs with high traffic intensity so far.

```

Initialize
For each iteration = 1:Ndo
  For each step = 1:Ldo
    For each ant = 1:K do
      Add a component to the solution based on transition rule
      Local updating for pheromone
    End
  End
  Global updating for pheromone
End
    
```

Fig. 6. The general structure of the ACS.

The difference between the state transition rule of our paper and the AS model is in the manner of controlling the influence of heuristic information in changing the position of the ants. We control the influence of heuristic information at the state transition rule by a matrix in which its elements have been selected according to the heuristic matrix elements. Thus the pixels that their change in local intensity in neighborhood is higher, have a greater share in the state transition rule with respect to the other pixels, so the movement of ants will be directed towards these pixels. In the presented paper, we use  $\beta_{\max}$  for pixels that have the higher change in their intensity more than a threshold and we use  $\beta_{\min}$  for the rest of the pixels. This statement is given by (12).

$$\beta_{ij} = \begin{cases} \beta_{\max} & \text{if } \eta_{ij} \geq \text{Threshold} \\ \beta_{\min} & \text{if } \eta_{ij} < \text{Threshold} \end{cases} \quad (12)$$

Where, the threshold is selected by the designer,  $\beta_{\max}$  is the maximum of weighting factor in heuristic information,  $\beta_{\min}$  is the minimum of weighting factor in heuristic information,  $\eta_{ij}$  is the heuristic information value of pixel at  $(i, j)$ .

According to the above comments, the state transition rule in our paper is shown in (13) in which the influence of the heuristic information is controlled by a matrix  $\beta$  instead of constant  $\beta$ .

$$P_{(i_0, j_0), (i, j)}^{(n)} = \frac{(\tau_{ij}^{(n-1)})^\alpha (\eta_{ij}) (\beta_{ij})}{\sum_{(i, j) \in \Omega_{(i_0, j_0)}} (\tau_{ij}^{(n-1)})^\alpha (\eta_{ij}) (\beta_{ij})} \quad (13)$$

Where,  $(i_0, j_0)$  is the current position of the ant;  $(i, j)$  is the next position for the ant;  $\tau_{ij}$  is the pheromone value for pixel  $(i, j)$ ;  $\Omega_{(i_0, j_0)}$  is the neighborhood pixels of pixel  $(i_0, j_0)$ ;  $\eta_{ij}$  is the heuristic information at pixel  $(i, j)$ ; and the constants  $\alpha$  and  $\beta$  control the influence of the pheromone and the heuristic information, respectively.  $\sum_{(i, j) \in \Omega_{(i_0, j_0)}} (\tau_{ij}^{(n-1)})^\alpha (\eta_{ij})^\beta$  is a normalization factor to limits the values of  $P_{(i_0, j_0), (i, j)}^{(n)}$  in  $[0, 1]$ .

The local update rule that is used in the presented paper is similar to the local update rule of ACS model. According to this rule, each ant when moving from one pixel to another, updates the pheromone value of the arcs that they pass through by (14).

$$\tau_{ij}^{(n)} = (1 - \varphi) \tau_{ij}^{(n-1)} \quad (14)$$

Where,  $\varphi \in (0, 1]$  is the pheromone decay coefficient;  $\tau_{ij}$  is the pheromone value that is assigned to the pixel at  $(i, j)$ .

Each ant is considered to have a memory in order to avoid local convergence. The address of the pixels that is visited by each ant is saved in its memory to prevent the repetitive movement of ants.

In the each iteration, after all ants finished L construction steps, the global update is performed on the pheromone. In ACS, the global update is done for the best result whereas in the presented paper the global update is performed for all of the visited pixels. This is due to the fact that some of the details in ACS algorithm are not suitable for the edge detection problem. Originally, the ACO is made to solve the TSP and in the TSP each ant produces a complete solution but in edge detection the aim of the ants is not to produce a complete solution but each of them has a share in edge detection. Therefore, as the nature of the ACO technique applied to the TSP is different from the nature of the ACO edge detection technique described in this paper it is needed that ACO with a little changes to be used where one of this changes is updating all the visited pixels instead of updating the best results. The global updating process is expressed in (15).

$$\tau_{ij}^{(n)} = (1 - \rho) \tau_{ij}^{(n-1)} + \rho \cdot \Delta \tau_{ij} \quad (15)$$

Where,  $\rho \in (0, 1]$  is the pheromone evaporation rate;  $\Delta \tau_{ij}$  is the quantity of pheromone laid on arc  $(i, j)$  and is equal to:

$$\Delta \tau_{ij} = \begin{cases} \frac{\sum_{k=1}^K \sum_{l=1}^L V_c(I_{ij})}{K} & \text{if } (i, j) \text{ is visited by an ant} \\ 0 & \text{otherwise} \end{cases} \quad (16)$$

Where, K is the number of ants; L is the number of construction steps;  $V_c(I_{ij})$  is the quantity of heuristic information of pixel at  $(i, j)$ .

At the end of iterations, we have a pheromone matrix that represents the edge information at each pixel and it can be used in order to extract edges.

### 3.3. Intelligent Thresholding

Using thresholding, one can extract the edges from the final pheromone matrix. There are several methods for thresholding such as classical thresholding in which a number is selected as a threshold and then all elements of pheromone matrix are divided into two groups due to the fact that each element can have the value higher or lower than the threshold. A thresholding technique called Otsu technique is introduced [22], and used in [21], [23]. In thresholding technique Otsu, the initial threshold  $T^{(0)}$  is selected as the mean value of the pheromone matrix. Then the matrix as explained is divided in two groups according to whether or not it is higher or lower than the threshold  $T^{(0)}$  so that the new threshold is computed as

the average of two mean values of each of the above two groups. The above procedure is repeatedly carried out until the successive threshold values  $T^{(n)}$  and  $T^{(n-1)}$  is almost the same (where the tolerance is defined by the user). In the final pheromone matrix, many of the pixels at background and adjacent pixels of edge pixels have the value of the pheromone near to the value of the pheromone for the edge pixels; therefore by using a classical thresholding those pixels are represented as an edge too. For the above reason in this paper, an intelligent thresholding technique is proposed to utilize the capabilities of neural network. This innovation causes to be able to extract maximum number of the edges. It is necessary to train a neural network to make an intelligent threshold. The neural network training and training patterns are described in the following.

A three layer neural network with 9-20-1 structure is used. The training algorithm that is used is the Back Propagation (BP) type and transfer function used for all neurons is the sigmoid type. The final pheromone matrix that is used as the input for neural network is used to create the target matrix. Using of masks  $5 \times 5$  reduces to zero value of the pheromone of the singular or the discontinuous points that have the value of pheromone greater than a threshold defined by the designer. Moreover, human observer performed the thinning operation to create an optimal target matrix. Input range for neural network is in the interval  $[0,255]$  and its outputs have only values of  $\{0, 1\}$ . Network training operation is performed for the standard image of the woman and its convergence profile is shown in Fig. 7. As seen in Fig. 7, network convergence profile is acceptable, therefore after training, it can be used for intelligent thresholding on the pheromone matrix of different images. Experimental simulating results demonstrate the ability of this thresholding method.

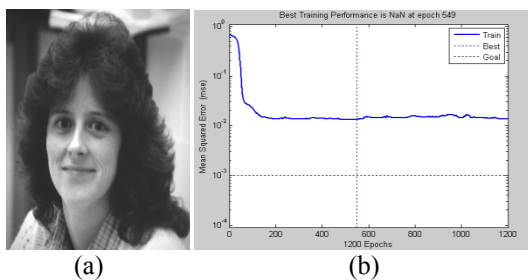


Fig. 7.(a) The original image of the woman, (b) The network convergence characteristic.

#### 4. EXPERIMENTAL RESULT

In experiments, initially, we are considering the performance of FIS that is presented for noise reduction. The FIS has been tested on the standard images of Rice, Barbara, Lena, Peppers and Cameraman that has been damaged by the salt and

pepper noise with the density of 15% and 20%. For the comparison, the presented method in [5] and standard median filtering method are tested in the same conditions. A criterion that is considered in evaluating the performance of the proposed method is the Power of Signal to Noise Ratio (PSNR) that is calculated by (17).

$$PSNR_{dB} = 10 \log_{10} \left( \frac{255^2}{\frac{1}{M \times N} \sum_{i=1}^M \sum_{j=1}^N (I_{ij} - \hat{I}_{ij})^2} \right) \quad (17)$$

Where,  $M \times N$  is the size of image;  $I_{ij}$  and  $\hat{I}_{ij}$  are value of pixel at  $(i, j)$  in noisy image and restored image, respectively.

Results for PSNR that are obtained from the proposed method and two other methods are listed in Table. 3. Comparing these results shows the efficient performance of fuzzy noise reduction method.

Table 3. PSNR (dB) is for various methods of noise reduction in noisy condition with the noise density of 15% and 20%

		Proposed approach	Approach In [5]	Median 3x3
15% salt & pepper	Cameraman	25.0652	24.9317	24.9238
	Lena	28.7300	28.1612	28.3102
	Rice	29.6845	27.9219	28.7639
	Peppers	29.8102	27.7795	29.0340
	Barbara	23.2924	24.6688	23.1645
20% salt & pepper	Cameraman	23.7873	22.4168	23.7030
	Lena	26.8957	25.2130	26.6622
	Rice	27.2162	24.2105	26.7146
	Peppers	27.0815	24.2498	26.7363
	Barbara	22.6121	22.4112	22.5183

We tested the proposed method on several standard images to evaluate its overall performance. Results for two images Lena and Peppers are shown in Table.4 and Table.5, respectively. Various parameters of the proposed method are chosen as follows:

- Iteration number =7: total number of the construction-process.
- Ant number =512: total number of ants.
- Step number = 200: total number of ant's movement-steps within each construction-process.
- Threshold=0.125: the threshold value in (12).
- $\rho = 0.1$ : the pheromone evaporation rate in (15).
- $\varphi = 0.05$ : the pheromone decay coefficient in (14).
- $\beta_{min} = 0.1$ : the minimum of weighting factor in the heuristic information in (12).
- $\beta_{max} = 2$ : the maximum of weighting factor in the heuristic information in (12).

- $\tau_{min} = 0.00001$ : the minimum of initial value of each component in the pheromone matrix.
- $\tau_{max} = 0.9$ : the maximum of initial value of each component in the pheromone matrix.
- $\alpha = 1$ : the weighting factor of the pheromone information in (13).

These values are chosen in such a way that the best results are obtained. These parameters are very effective for the result of the proposed method and are chosen by trial and error method. Fig. 8 shows the importance of choosing the values for these parameters.

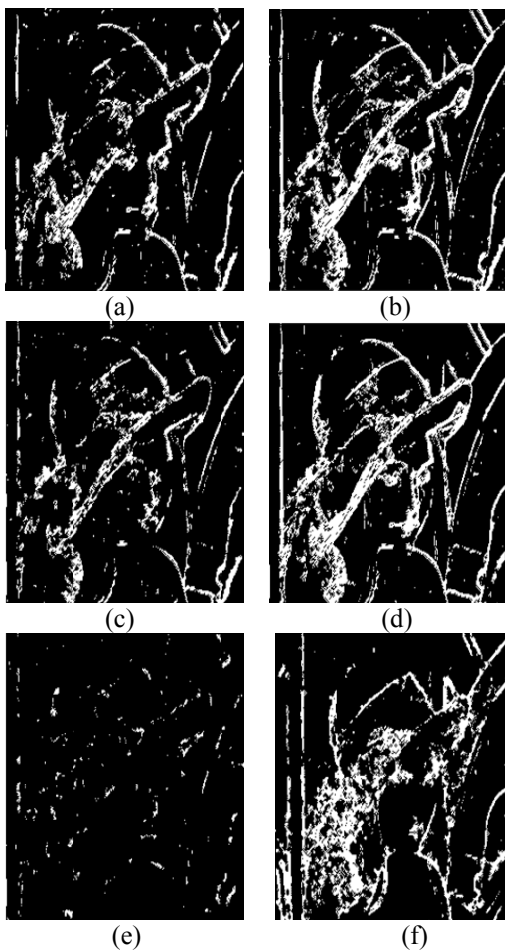


**Fig. 8.** Resulted images from changing of parameter's value, (a)  $K=256$ , (b)  $K=768$ , (c)  $L=40$ , (d)  $L=400$ , (e)  $\rho = 0.9$ , (f)  $\varphi = 0.2$ .

Results of the performance of Sobel and Canny and the result of the method that is presented in [21] are given in order to compare them with the results presented in the paper which confirms the performance of the presented method. As can be seen, although previous works have acceptable performance in noise-free conditions, but their response is unacceptable in







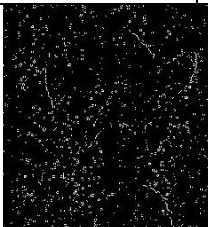
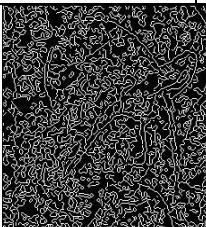
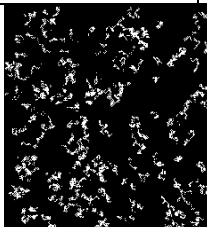

terms of the noise. However the response of the proposed method in this paper is acceptable in both noise-free and noisy conditions. We have provided these results by using a simple noise reduction step and conducting ant's algorithm. In noisy conditions, the superiority of the obtained response to the presented method in this paper is well illustrated and in noise-free condition it should be said that the method in our paper can extract more edges than the method in [21] and also in comparison with the Sobel and Canny performances, our method has been able to extract more edges with the better quality. Note that the proposed method is designed only for edge detection of noisy images that have been degraded by salt and pepper noise, but in future works we can develop a fuzzy system to filter all kinds of noise. We know the proposed method for edge detection is based on ACO, therefore, it is valuable to compare the results of proposed method with the results of other methods based on ACO and demonstrate the performance of the proposed method. Table. 6 shows the results of proposed method and other methods. To provide a fair comparison, edge detection is done for noise-free conditions because other methods have been proposed for noise-free condition.

## 5. CONCLUSION







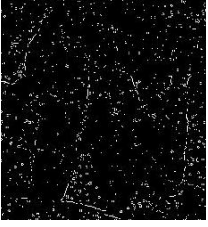
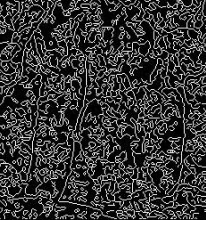
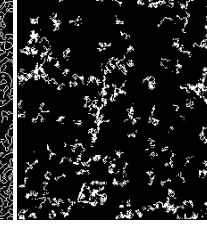

In this paper, a new method is presented for edge detection of noisy images that is degraded by salt and pepper noise. It uses the intelligent techniques. We have been able to provide a robust noise reduction by using a simple fuzzy system that leads to obtain the noise free images with considerable PSNR. Then, we have detected the probable edge pixels in 4 main directions and this identification in conduction of the ant's movement is used in ACO. In ACO, we can conduct the movement of ants toward edges further and we increase the ACO convergence by increasing the influence of edge pixel that is detected by fuzzy system and by increasing the influence of pixels that have greater change in intensity at their local neighborhood. Finally, we could extract the edges of the final pheromone matrix by introducing an intelligent thresholding technique. Simulation results show that the presented method in our paper has been able to extract more edges with the better quality than the other methods in both noisy and noise-free conditions. As for the future works, one can design intelligent ants which themselves have the ability to identify and distinguish the edge and noisy pixels and don't release the pheromone on the noisy pixels.







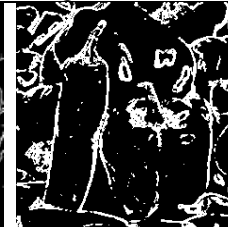




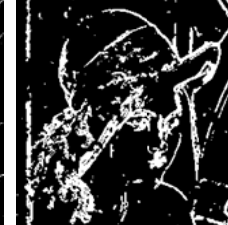
**Table 4.** Edges images obtained using various methods for original image of Lena and noisy image of Lena.

	Image of Lena	Sobel	Canny	Method in [21]	Proposed method
Result for edge detection of original image					
Result for edge detection of noisy image					

**Table 5.** Edges images obtained using various methods for original image of Peppers and noisy image of Peppers.

	Image of Peppers	Sobel	Canny	Method in [21]	Proposed method
Result for edge detection of original image					
Result for edge detection of noisy image					

**Table 6.** Original images and the test results of various edge detection methods based on ACO.

Image of Peppers	Method in [23]	Method in [24]	Method in [25]	Proposed method
				
				

## REFERENCES

- [1] H. Hassanpour, E. Nadernejad, and H. Miar, "Image restoration using a PDE-based approach," *Int. J. of Engineering- Trans.B:Applications,Ar.*, Vol. 20, No. 3, pp. 225-236, Dec.2007.
- [2] E. Nadernejad and H. Hassanpour, "A comparison and analysis of different PDE-based approaches for image enhancement," in *Proc. Int. Conf. on Signal Processing and Communication Systems ICSPCS*, Australia, Dec.2007.
- [3] R. C. Gonzalez and R. E. Woods, *Digital Image Processing*, Prentice Hall, 2004.
- [4] T. Chen, K. K. Ma, and L. H. Chen, "Tri-State Median Filter for Image Denoising," *IEEE Transactions on Image Processing*, Vol. 8, No. 12, pp.1834-1838, Dec.1999.
- [5] V. Crnojevic, V. Senk, and Z. Trpovski, "Advanced Impulse Detection Based on Pixel-Wise MAD," *IEEE Signal Processing Letters*, Vol. 11, No. 7, pp. 589-592, July. 2004.
- [6] R. Garnett, T. Huegerich, C. Chui, and W. He, "A Universal Noise Removal Algorithm With an Impulse Detector," *IEEE Transactions on Image Processing*, Vol. 14, No. 11, pp. 1747-1754, November. 2005.
- [7] P. Kumar Sa, B. Majhi, G. Panda, "Improved Adaptive Impulsive Noise Suppression," *Fuzzy Systems Conference. 2007*, Fuzz-IEEE 2007. IEEE International.
- [8] C. J. Miosso, and A. Bauchspiess, "Fuzzy Inference System Applied to Edge Detection in Digital Images," *Proceedings of the V Brazilian Conference on Neural Networks*, pp. 481-486, April. 2001.
- [9] L. Hu, H. D. Cheng, and M. Zhang, "A High Performance Edge Detector Based On Fuzzy Inference Rules," *Information Science 177*, pp. 4768-4784, 2007.
- [10] J. K. Paik, and A. K. Katsaggelos, "Edge Detection Using A Neural Network," *International Conference on Acoustics, Speech, and Signal Processing, ICASSP- 90*, pp. 2145- 2148, April. 1990.
- [11] M. S. Bhuiyan, H. Matsuo, A. Iwata, H. Fujimoto, and M. Sato, "An Improved Neural Network Based Edge Detection Method," Tech. Rep., Dept. of Electrical and Computer Engineering and Dept. of Mechanical Engineering, Nagoya Institute of Technology, Nagoya, JAPAN 466.
- [12] M. Dorigo, G. D. Caro, and T. Stutzle, "Special Issue on Ant Algorithms," *Future Generation Computer Systems*, Vol. 16, Jun.2000.
- [13] O. Cordon, F. Herrera, and T. Stutzle, "Special Issue on Ant Colony Optimization: Models and Applications," *Mathware and Soft Computing*, Vol. 9, Dec. 2002.
- [14] M. Dorigo, L. M. Gambardella, M. Middendorf, and T. Stutzle, "Special Issue on Ant Colony Optimization," *IEEE Transactions on Evolutionary Computation*, Vol. 6, Jul. 2002.
- [15] H. Zheng, A. Wong, and S. Nahavandi, "Hybrid ant colony algorithm for texture classification," in *Proc. IEEE Congress on Evolutionary Computation, Canberra, Australia*, pp. 2648-2652, Dec. 2003.
- [16] D. Martens, M. D. Backer, R. Haesen, J. Vanthienen, M. Snoeck, and B. Baesens, "Classification with ant colony optimization," *IEEE Trans. on Evolutionary Computation*, Vol. 11, pp.651-665, Oct.2007.
- [17] A. T. Ghanbarian, E. Kabir, and N. M. Charkari, "Color reduction based on ant colony," *Pattern Recognition Letters*, Vol. 28, pp.1383-1390, Sep.2007.
- [18] M. Dorigo, and T. Stutzle, *Ant Colony Optimization*, Cambridge: MIT Press, 2004.
- [19] M. Dorigo and L. M. Gambardella, "Ant Colony System: a cooperative learning approach to the traveling salesman problem," *IEEE Trans. on Evolutionary Computation*, Vol. 1, pp. 53-66, Apr.1997.
- [20] T. Stutzle, and H. Holger H, "Max-Min ant system," *Future Generation Computer Systems*, Vol. 16, pp. 889-914, Jun.2000.
- [21] J. Tian, W. Yu, S. Xie, "An Ant Colony Optimization Algorithm For Image Edge Detection," *IEEE Congress on Evolutionary Computation*, pp. 751-756, June. 2008.
- [22] N. Otsu, "A threshold selection method from gray level histograms," *IEEE Trans. Syst. Man, Cybern*, Vol. 9, pp.62-66, Jan.1979.
- [23] A. V. Bateria, C. Oppus, "Image edge detection using ant colony optimization," *WSEAS Transactions on Signal Processing*, Issue. 2, Vol. 6, pp. 58-67, Apr. 2010.
- [24] H. Nezamabadi-pour, S. Saryazdi, and E. Rashedi, "Edge detection using ant algorithms," *Soft Computing*, Vol. 10, pp. 623-628, May. 2006.
- [25] J. Zhang, K. He, X. Zheng, J. Zhou, "An Ant Colony Optimization Algorithm for Image Edge Detection" *International Conference on Artificial Intelligence and Computational Intelligence (AICI)*, Conference Publications, Vol. 2, pp. 215-219, Oct. 2010.